Radiography 30 (2024) 986–994

Contents lists available at ScienceDirect

Radiography

journal homepage: www.elsevier.com/locate/radi

Predictive value of magnetic resonance imaging diffusion parameters using artificial intelligence in low-and intermediate-risk prostate cancer patients treated with stereotactic ablative radiotherapy: A pilot study

A. Kedves [a, b, c], M. Akay [d], Y. Akay [d], K. Kisiván [a], C. Glavák [a], Á. Miovecz [a, c], Á. Schiffer [b], Z. Kisander [e], A. Lőrincz [b, f], A. Szőke [j], B. Sánta [g], O. Freihat [k], D. Sipos [a, h], Á. Kovács [c, h, i], F. Lakosi [a, c, h, *]

[a] "Moritz Kaposi" Teaching Hospital, Dr. József Baka Diagnostic, Radiation Oncology, Research and Teaching Center, Kaposvár, Hungary
[b] Institute of Information and Electrical Technology, Faculty of Engineering and Information Technology, University of Pécs, Pécs, Hungary
[c] Doctoral School of Health Sciences, University of Pécs, Pécs, Hungary
[d] Department of Biomedical Engineering, University of Houston, Houston, TX, USA
[e] Department of Electrical Networks, Faculty of Engineering and Information Technology, University of Pécs, Pécs, Hungary
[f] Institute for Translational Medicine, Medical School, University of Pécs, Pécs, Hungary
[g] Röntgenpraxis Dr. Thomas Trieb, Innsbruck, Austria
[h] Institute of Diagnostics, Faculty of Health Sciences, University of Pécs, Pécs, Hungary
[i] Department of Oncoradiology, Faculty of Medicine, University of Debrecen, Debrecen, Hungary
[j] 3D Printing and Visualization Centre, Medical School, University of Pécs, Pécs, Hungary
[k] College of Health Sciences, Abu Dhabi University, Abu Dhabi, UAE

ARTICLE INFO

Article history:
Received 12 September 2023
Received in revised form
25 March 2024
Accepted 28 March 2024
Available online 27 April 2024

Keywords:
ADC
Machine learning
Multiparametric
Predictive
Prostate cancer
Prediction models
SABR

ABSTRACT

Introduction: To investigate the predictive value of the pre-treatment diffusion parameters of diffusion-weighted magnetic resonance imaging (DW-MRI) using artificial intelligence (AI) for prostate-specific antigen (PSA) response in patients with low- and intermediate-risk prostate cancer (PCa) treated with stereotactic ablative radiotherapy (SABR).

Methods: Retrospective evaluation was performed for 30 patients using pre-treatment multi-parametric MR image datasets between 2017 and 2021. MR-based mean- and minimum apparent diffusion coefficients (ADC_{mean}, ADC_{min}) were calculated for the intraprostatic dominant lesion. Therapeutic response was assessed using PSA levels. Predictive performance was assessed by the receiver operating characteristic (ROC) analysis. Statistics performed with a significance level of $p \leq 0.05$.

Results: No biochemical relapse was detected after a median follow-up of twenty-three months (range: 3–50), with a median PSA of 0.01 ng/ml (range: 0.006–2.8) at the last examination. Significant differences were observed between the pre-treatment ADC_{mean}, ADC_{min} parameters, and the group averages of patients with low and high 1-year-PSA measurements ($p < 0.0001$, $p < 0.0001$). In prediction, the random forest (RF) model outperformed the decision tree (DT) and support vector machine (SVM) models by yielding area under the curves (AUC), with 0.722, 0.685, and 0.5, respectively.

Conclusion: Our findings suggest that pre-treatment MR diffusion data may predict therapeutic response using the novel approach of machine learning in PCa patients treated with SABR.

Implications for practice: Clinicians shall measure and implement the evaluation of the suggested parameters (ADC_{min}, ADC_{mean}) to provide the most accurate therapy for the patient.

Abbreviations: AI, artificial Intelligence; ADC, apparent diffusion coefficient; DT, decision tree; AUC, area under the curves; DW-MRI, diffusion-weighted magnetic resonance imaging; PCa, prostate cancer; PSA, prostate specific antigen; RF - [not related to coil radiofrequency], random forest; ROC, receiver operating characteristic; SABR, (prostate) stereotaxic ablative radiotherapy.

* Corresponding author. "Moritz Kaposi" Teaching Hospital, Dr. József Baka Diagnostic, Radiation Oncology, Research and Teaching Center, Kaposvár, Hungary.
E-mail address: lakosiferenc@yahoo.com (F. Lakosi).

https://doi.org/10.1016/j.radi.2024.03.015

Introduction

Prostate cancer (PCa) is still the most prevalent and second-deadliest disease among males in the United States, with an incidence of 117 cases per 100,000 men and 19 deaths per 100,000 men, both age-standardized to the US standard population of 2000.[1]

The final treatment options for prostate cancer are determined by a patient's risk, which is determined by prostate-specific antigen (PSA) level, clinical T-stage, Gleason pattern, and the number of cores positive, according to risk stratification.[2,3] While it would take more time to evaluate the long-term outcomes of PSA follow-up, studies on early responses have been conducted, which could provide valuable insights into the kinetics of prostate cancer and alternative treatment approaches.[4,5]

The technical development of radiation therapy has enabled prostate stereotaxic ablative radiotherapy (SABR), which delivers high doses with high precision, in a low (≤10) fraction number, with targeted inhomogeneity to target volumes.[6–8] As a result, the number and indications of SABR treatments constantly expand worldwide.[9–11]

In patients with PCa, the use of SABR has been connected to improved progression-free survival and overall survival,[11–15] might yield less local failure than multifraction, costs less,[16,17] and appeared to result in a satisfactory quality of life (QOL).[18–20] Furthermore, compared to focal-cryoablation, SABR is associated with equivalent oncologic and functional results.[21] These findings highlight the value of SABR in treating PCa with low-to intermediate-risk.

For the detection and characterization of PCa, diffusion-weighted magnetic resonance imaging (DW-MRI) is a viable imaging biomarker.[22,23] Additionally, it has been demonstrated that the use of DW imaging (DWI) and its measurement using the apparent diffusion coefficient (ADC) increases the sensitivity of PCa detection.[24,25] In PCa, cancerous cells tend to exhibit a more restricted diffusion of water molecules compared to normal prostate tissue, leading to lower ADC values in tumor-affected regions. Overall, ADC plays a crucial role in the modern diagnosis, characterization, and prognostication of PCa, contributing to improved patient management and treatment decisions. However, it is still unknown whether pre-treatment ADC can be used to predict short-term outcomes following SABR in PCa.

The complexity and non-linearity of biological systems are inherent.[26] Thus, artificial intelligence (AI) based non-linear predictions in patients treated with various indications[27–29] and in PCa[24,30,31] are widely used among researchers.

AI includes a branch called machine learning (ML) in which computers are programmed to recognize patterns in data. The learning process is based on mathematical guidelines and statistical presumptions.[32] In addition, the medical industry has quickly developed and applied it, particularly when creating predictive models.[33] As a result, it would be practical and promising to develop PCa prediction models using machine learning.

The use of tree models[34] and random forests-which are computationally quick - are frequently used as effective and efficient solutions for feature selection in assessing the preoperative status and further diagnosis of PCa,[35] predicting lymph node involvement[36] or even for drunk driving recognition.[37] Additionally, alternative prediction techniques, such as the support vector machine (SVM), could work effectively on a sample with fewer elements.[38]

This study aimed to determine the best predictors for the biochemical response of patients diagnosed with MR-DWI using supervised machine learning methods. Additionally, this study sought to assess the relationship between the potential variables that turned out to be the most accurate predictors of the outcome of PCa.

Materials and methods

Patients

Between January 2017 and December 2021, 40 low- and intermediate-risk PCa (National Comprehensive Cancer Network criteria [NCNN], [IRPCa]) patients were treated with SABR in “Moritz Kaposi” Teaching Hospital, Dr. József Baka Diagnostic, Radiation Oncology, Research and Teaching Center, Kaposvár, Hungary and enrolled to our study.

Patient characteristics are summarized in Table 1. Serum total prostate-specific antigen (tPSA) > 4 ng/ml, abnormal digital rectal exam, or imaging findings suggestive of suspected prostate cancer were all reasons for prostate biopsy. The histopathology review consisted of 10–12 cores of systematic biopsy performed on all patients for staging. Ineligibility criteria were the following: (1) a high (>18) International Prostate Symptom Score (IPSS), (2) prostate volume >100 cc, (3) inflammatory bowel disease. Patients with image artefacts, especially DWI sequences, or those unable to complete the therapy for any reason were excluded from the study.

Treatment

Prostate SABR was introduced after national and local ethical committee approvals (OGYEI: 5838/2017, 66793/2018, 69293/2017), and informed consent was obtained from all subjects and/or their legal guardian(s). Low-risk (LR) and intermediate-risk (IR) patients were treated with VMAT-based SABR monotherapy, with a total dose of 36.25 Gy in five fractions (fx).

For each patient before treatment, three gold seeds (1 mm × 3 mm, [CP Medical, Portland, USA]) were implanted into the prostate. Treatment verification consisted of pre-and post radiation therapy (RT) cone-beam computed tomographies (CBCT), with online gold marker-based triggered kilovoltage imaging with auto beam hold. In case of ≥3 mm displacement, the treatment was interrupted, and an imaging-based correction was performed.[39]

Imaging

Examinations were performed using a 3.0 T MRI scanner (Biograph mMR, Siemens Healthcare GmbH., Erlangen, Germany).

Table 1
Patient and tumor characteristics. *initial prostate-specific antigen (iPSA) * ISUP International Society of Urological Pathology.

Characteristics	Value (%/range)
Number of patients	30 (100%)
Median age (year)	68 ± 7.4 (48–83)
T stage,[a] N	
1c	20 (66.6%)
2a	6 (20%)
2b	4 (13%)
iPSA, ng/ml, mean	8.52 ± 3.57 (1.2–17)
1-year-PSA, ng/ml, mean	0.53 ± 0.58 (<0.003–1.91)
Gleason Score, mean	6.35 ± 0.53 (5–7)
Mean gland volume (cm^3)	41.72 ± 18.34 (8–92)
Risk group	
Low risk	12 (40%)
Intermediate risk	18 (60%)
ISUP grade	
1	18 (60%)
2	11 (36.6%)
3	1 (3.4%)
Follow-up (month)	23 (3–50)

[a] Based on clinical (American Joint Committee on Cancer Staging System, 8th edition) and pelvic MRI stage *pts patients.

After a localizer, T2-weighted turbo spin echo (TSE) sagittal (TR/TE/FA 4200/133 ms/120°, FOV: 240 mm, slice thickness: 3 mm, 256 × 256) and T2-weighted TSE transversal (TR/TE/FA 6500/106 ms/149°, FOV: 240 mm, slice thickness: 3 mm, 320 × 320) images. In addition, T2-weighted TSE coronal (TR/TE/FA 3700/133 ms/120°, FOV: 240 mm, slice thickness: 3 mm, 256 × 256) and T1 TSE transversal (TR/TE/FA 700/9.3 ms/110°, FOV: 200 mm, slice thickness: 3 mm, 256 × 256) images were acquired.

DW MRI measurement was done as part of a routine examination. In this case, a 2D spin-echo DWI echo-planar (EP) sequence (FOV: 315 mm, TR: 5000 ms, TE minimum: 72 ms, TI 200 ms, FA: 90°, slice thickness: 3 mm) was used. First, the implemented software automatically generated an ADC map from the DWI pictures. Then, the restricted diffusion rate was quantified by calculating the apparent diffusion coefficient. A 100 s/mm2 "b" value was used as the first measurement (the other b values were 800 s/mm^2, 1500 s/mm^2, and 2000 s/mm^2) to reduce the perfusion effect on the ADC calculation.

Furthermore, a T1-weighted TSE axial sequence (TR/TE/FA 700/9.3 ms/85°, FOV: 200 mm, slice thickness: 3 mm, 256 × 256) and a T1-weighted TSE StarVIBE FS transversal sequence (TR/TE/FA 3.83/1.75 ms/9°, FOV: 200 mm, slice thickness: 3 mm, 320 × 320, with an isotropic resolution of 1 mm^3) were conducted after 0.1 mmol per kg of bodyweight contrast material (Gadovist© Bayer Healthcare, Leverkusen, Germany) was injected into the patient. Despite the fact that dynamic contrast-enhanced and T1-weighted images were created for clinical assessments, this study only checked for false positive cases.

Using the eRAD PACS Desktop Viewer 8.0 program, the location of lesions was evaluated on the ADC map. We selected the tumor's prominent and most homogeneous part as a benchmark for all entities in this investigation, which used the single-slice measuring approach.[40] The Region of Interest (ROI) was manually placed on the most solid part of the tumor, which has the highest signal intensity on DWI pictures (hyperintense), the lowest signal intensity on the ADC map,[41,42] and T1-weighted imaging can be used to prevent false-positive T2-weighted imaging results.[43,44] (Fig. 1). ADC_{mean} and ADC_{min} were used as standard measurement units to reduce the impact of tumor heterogeneity in all lesions. In the case of ADCmean we used the average ADC of the overall area included in the ROI which is calculated automatically by the software, where "Avg" represents the average ADC values for all voxels within the ROI and "Dev" Represents the standard deviation. These were also the standard units to be used as a reliable parameter because they reflected the tumor heterogeneity in the given slice and allowed the researcher to distinguish the various entities in the same image.[42,45] ROI measurements were performed by a trained radiographer.

Clinical evaluation

We aimed to evaluate the 1-year PSA response, meaning that we looked at 1-year outcomes for all patients. Thus, based on the median value, two patient groups were created by normalizing the ratio of the 1-year measured PSA value to the baseline PSA, which reflects the rate of decline. Accordingly, a "low PSA group" and a "high PSA group" were established.

A radiation oncologist evaluated and recorded IPSS, and measured PSA levels throughout follow-up to illustrate kinetics, and other patient-related data were collected.

Model development, statistical analysis

Python scripts and in-house machine learning models (decision tree [DT], random forest [RF], and SVM) based on the Python software environment for statistical computing (version 3.8; Python Software Foundation, Beaverton, OR) were used following the guidelines of NumPy, SciPy, seaborn, and scikit-learn software packages for statistical analyses carried out. Circos scripts developed in Matlab software environment (MATLAB. [2022]. Version R2022a. Natick, Massachusetts: The MathWorks Inc.) using schemaball add-on.

For the DT our code uses the DecisionTreeClassifier class from scikit-learn to create a decision tree classifier object. The fit() method is then used to train the classifier on the input data. Finally, the predict() method is used to predict the response to new observations. In the case of RF, Scikit-learn's RandomForestClassifier class was used to generate a random forest classifier object. The classifier is then trained using the fit() function on the input data. Finally, the predict() technique is employed to forecast the outcome of fresh observations. In the instance of SVM, code uses the SVC class from scikit-learn to create a support vector machine classifier object with a linear kernel and regularization parameter. The fit() method is then used to train the classifier on the input data. Finally, the predict() method is used to predict the response to new observations.

In all of our models, scaling (via "StandardScaler") and cross-validation (via "cross_val_score") were done for the raw data. Because of using binary outputs, DT and RF classifier methods have been chosen ("DecisionTreeClassifier" and "RandomTreeClassifier," respectively). "sklearn.tree" has been split and utilized for training for the DT model. The RF model was trained and separated using the "sklearn.ensemble" function. SVM model performed via "sklearn.svm". Model filtered by radial basis function (RBF), setting the two hyperparameters, cost (C) and gamma, to 1 and 0.1, respectively. Models have been developed to determine the relative importance of each predictor candidate in the therapy response classification as measured by the Gini index.

Data analysis

A receiver operating characteristic (ROC) curve was made for the primary tumor ADC values to assess the predictive value of recurrence at any time with the maximum sensitivity and specificity. The area under the curve (AUC) was calculated during the ROC curve analysis. AUC must be at least 0.70 to be deemed fair.[46]

To check whether the measured ADC_{min}, ADC_{mean}, age, the volume of the prostate (volume), initial PSA (iPSA), and 1-year-PSA values were the normally distributed, the Shapiro–Wilks test[47] was utilized. The Wilcoxon rank-sum test was used to compare groups because these tests revealed non-normality distributions of the ADC_{min}, ADC_{mean}, Age, iPSA, Volume, and 1-year-PSA ($p < 0.0001$, $p < 0.0001$, $p = 0.0001$, $p < 0.0001$, $p < 0.0001$, $p < 0.0001$, respectively) in the population. Spearman's correlation coefficient was used to describe the strength of the correlation between the data pairs. Statistical significance was defined as p values less than 0.05.

Results

A total of 30 patients were enrolled in this study. The patients' characteristics are summarized in Table 1. There was no visible lesion for the remaining patients, or MRI was not evaluable due to previous neoadjuvant ADT or a contraindication for MRI. The mean ADCmean (+standard deviation [SD]) and ADCmin values were 781.34 ± 56.15 10^{-6} mm^2/s (range, 605.66–905.85), and 771.33 ± 45.15 10^{-6} mm^2/s (range, 602.82–898.41), respectively.

Correlation analysis

After a median follow-up of twenty-three months (range: 3–50), the median PSA nadir was 0.01 ng/ml (range: 0.006–2.8). No biochemical relapse has been detected so far. Although, 45% of

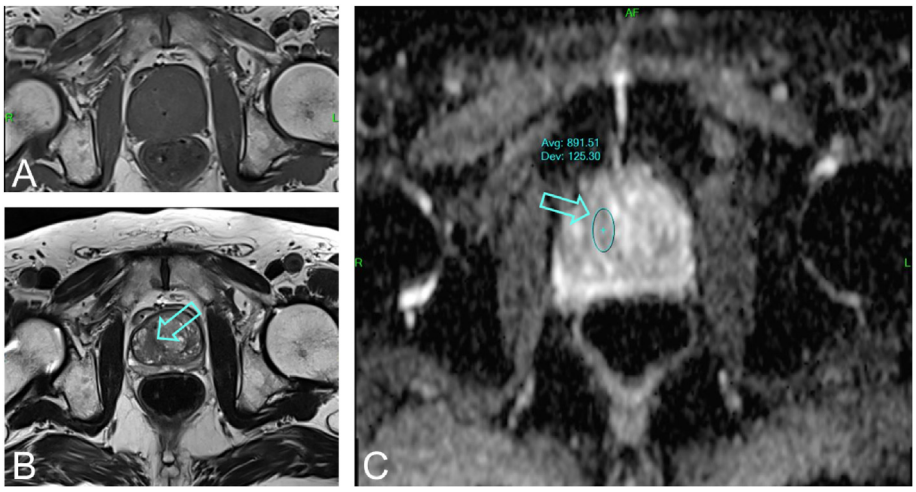

Figure 1. Axial T1-weighted TSE sequence (A) and axial T2-weighted TSE sequence (B) were used as an anatomical map. On the corresponding ADC map (C), the area of low signal intensity is shown and measured by the ellipsoid ROI (blue ellipse). The tumor is located in the right posterior transitional zone of the prostate on the right side. The 11 mm elongated proliferation with irregular borders (blue arrow) shows diffusion restriction (ADCmean: 891.51+-125.30 10-6 s/mm^2). *region of interest (ROI) * turbo spin echo (TSE) * apparent diffusion coefficient (ADC).

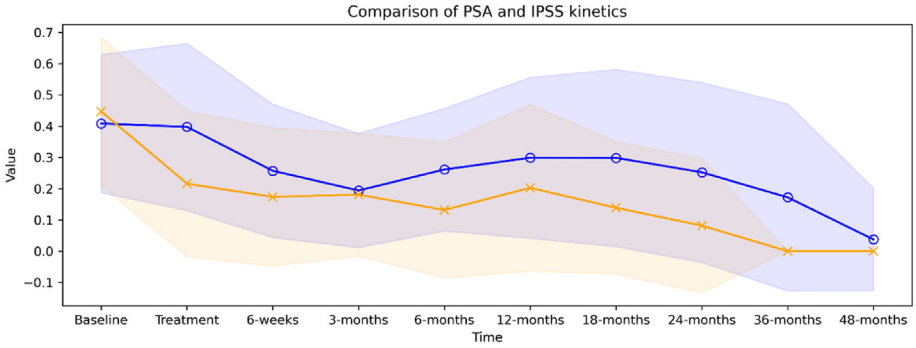

Figure 2. Plots represent rescaled average PSA values for patients 2 years after therapy (orange), while the blue color represents rescaled average IPSS values up to 42 months. The colored ribbons indicate standard deviations. *prostate-specific antigen (PSA) *International Prostate Symptom Score (IPSS).

patients have not yet reached their PSA nadir. The median time to PSA nadir was 17.6 months (range: 2–34).

The 3-month PSA value, PSA kinetics, and ADC values do not show significant correlations ($p > 0.05$). Rescaled average PSA values 2 years after the therapy and rescaled average IPSS values up to 42 months showed an overall decreasing trendline in PSA kinetics. Due to a lack of data, the PSA values are represented as zero after 24 months (Fig. 2).

Not statistically significant, but moderate negative correlations were found between ADCmean and age, and ADCmin and age ($r = -0.4412$, $\rho = -0.3762$ and $r = -0.4728$, $\rho = -0.3701$). Otherwise, no further relations were noted between age, iPSA, Volume, ADCmin, and the ADCmean. The results of the correlation analysis are summarized in Figs. 3–4, and Supplementary figure 1.

Via the Wilcoxon rank-sum test, the volume did not prove to be significant ($p = 0.1428$) (Supplementary figure 2), however group averages of subjects with low and high 1-year-PSA values showed statistically significant differences ($p < 0.0001$, $p < 0.0001$, respectively) (Fig. 5), without any further significance for the other parameters ($p > 0.05$).

Measured parameters, machine learning, and response

Due to the relatively low number of patients, the ML data of PC patients were classified into a training (70%) and a validation set

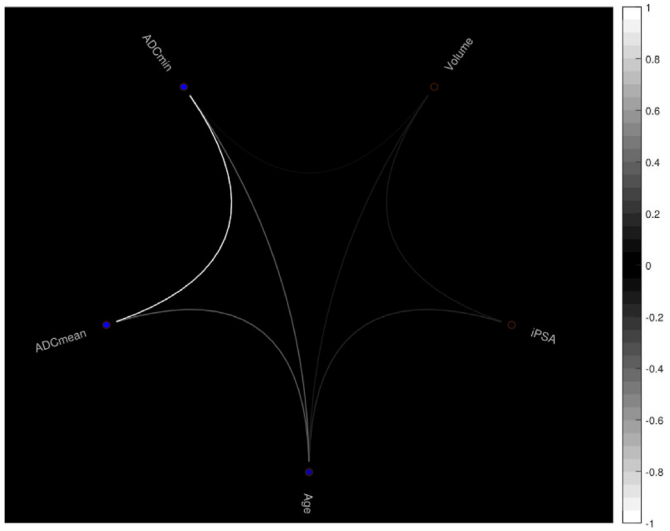

Figure 3. Circos based on the Spearman correlation coefficients matrix shows the correlation between the pre-treatment parameters. *Minimum Apparent Diffusion Coefficient (ADC_{min}) *Pre-treatment/Initial Prostate Specific Antigen (iPSA) *Mean Apparent Diffusion Coefficient (ADC_{mean}). *prostate-specific antigen (PSA).

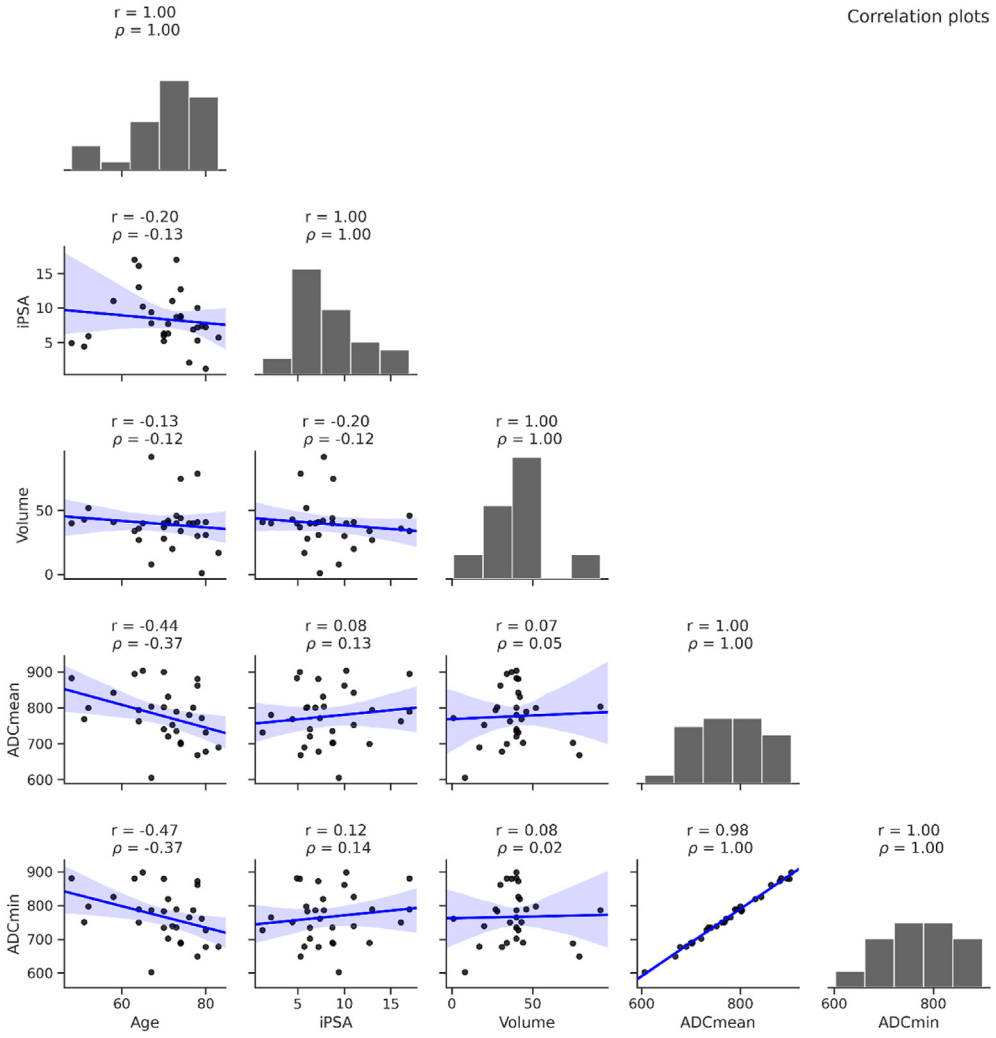

Figure 4. Correlation plots (linear regression along with 95% CI - lower triangle) with Spearman correlation coefficients and histograms (diagonal) are shown in the plot matrix of pre-treatment data. *Minimum Apparent Diffusion Coefficient (ADC_{min}) *Pre-treatment/Initial Prostate Specific Antigen (iPSA) *Mean Apparent Diffusion Coefficient (ADC_{mean}). *prostate-specific antigen (PSA) *confidence interval (CI).

(30%). As a result, the developed random forest model outperformed the decision tree and the support vector machine model in prediction, with corresponding areas under the curves (AUC) of 0.722, 0.685, and 0.5, respectively. Table 2 shows the performance of the RF model. The relative importance ranks of the features are in Fig. 6, whereas ADC_{min} ranked third. The process is visualized in Fig. 7.

Discussion

Overall, this study mainly focused on DWI imaging parameters' combined role in predicting biochemical response to therapy in PCa patients. After a 2-year median follow-up, no biochemical relapse was detected in our study, which compares favourably with the literature.[48,49] This retrospective analysis demonstrates correlations between baseline MRI-DWI-based measures (ADC_{min}, ADC_{mean}) and cancer-specific characteristics (iPSA, Volume) and emphasizes their influence on the therapeutic response (low 1-year-PSA- and high 1-year-PSA group). As an outcome of this study, we found that machine learning can be utilized to forecast the response of prostate cancer treated with SABR using MRI-DWI values.

Risk stratification is essential for selecting the best PCa treatment plan and forecasting patient outcomes. The most crucial prognostic markers for predicting the success of the therapy (e.g., biochemical failure [BF]) in patients after radical prostatectomy are pre-treatment PSA levels, clinical stage, and GS.[50] However, additional elements like RT dose, irradiation fields, and ADT were discovered to be connected to BF in patients who undergo definitive RT.[51,52] Thus, a detailed evaluation of the entire prostate is necessary before performing definitive RT, in which the staging is based on clinical and radiologic findings, and the histological evaluation is based primarily on prostate biopsy results. Therefore, non-invasive techniques may be a good alternative for assessing the whole prostate and tumor biology before RT. These were areas where DWI-MRI shows promise since it allows for examination of the entire prostate gland, significantly decreasing the chance of sampling error during a biopsy.

The quantification of tumors is made possible by DW-MRI calculations generated from ADC. A measure known as the apparent diffusion coefficient is a quantitative metric employed in MRI to assess the microstructure of tissue, particularly in the context of malignant prostate cancer. ADC measurements can be used to evaluate the aggressiveness of PCa, as higher ADC values are typically associated with lower tumor grade and a more favorable

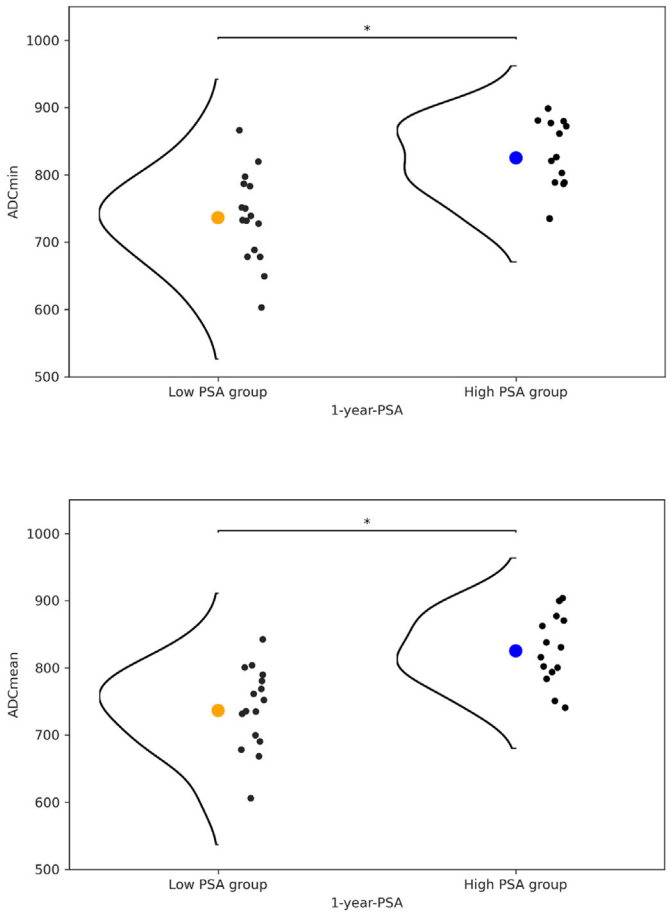

Figure 5. Violin-plots show the distributions of ADCmin (upper) and ADCmean (lower) parameters in the therapy response-based subgroups, patients who achieve low PSA group and high PSA group. The sample mean is indicated by the colored dot. The significant p-value of the Wilcoxon rank-sum test is denoted by a star. *Minimum Apparent Diffusion Coefficient (ADC_{min}) *Mean Apparent Diffusion Coefficient *(ADC_{mean}) Prostate Specific Antigen.

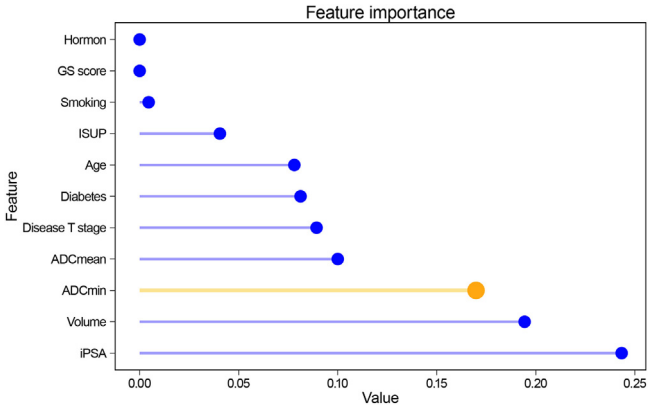

Figure 6. Feature importance plot of all relevant parameters (relative importance). Classification using a random forest identification of the features that could have the most significant effect on differentiating the study groups ordered according to their Gini coefficient. *Minimum Apparent Diffusion Coefficient (ADC_{min}) *Mean Apparent Diffusion Coefficient (ADC_{mean}). *Gleason score (GS), *Pre-treatment/Initial Prostate Specific Antigen (iPSA) *prostate-specific antigen (PSA).

prognosis. The presence of more cells, larger nuclei, more macromolecular proteins, and less extracellular space in malignant tumors may result in lower ADC readings.[53] In PCa patients, earlier research showed a negative correlation between ADC values and tumor aggressiveness,[54,55] which was also confirmed in our study. In addition, Chatterjee et al. discovered a negative correlation between GS and ADC values and lower ADC values in patients with high-risk characteristics such as a high serum PSA level, stage, or tumor grade, implying that ADC values could be used to predict prognosis.[56] Despite this earlier study, we found no relevant connection between tumor ADC values and early elevated blood iPSA levels in our SABR patient group; we only found a significant correlation with the 1-year post-therapy PSA. Onal et al. noted that patients who progressed had a lower mean ADC value than those who did not, with a considerably larger patient population ($n = 503$).[24] In our single-institute study, there was no progression. ADC plays a fundamental role in contemporary PCa diagnosis, characterization, and prognostication, contributing to enhanced patient management and treatment selection.

In our case, we had higher and lower 1-year PSA level groups. Interestingly, we observed a significant difference in ADC values between the two groups in our early, only after 1-year follow-up setting. Its predictive value needs to be confirmed by long-term clinical results. Utilizing them as a guide, we recognized a pattern that helped us identify the therapy result for our IRPCa patients throughout the shorter follow-up. Besides, not statistically significant, but moderate negative correlations were found between ADC and age, which is probably due to alteration in the cellular water with advancing age.

The ROC analysis in our study proved the clinical utility of the RF model, which outperforms the DT and SVM models. Dutta et al. found that the RF model can be used well to predict biochemical recurrence. In their study, they investigated different segmentation methods (manual, automatic) based radiomics and found that manual segmentation based features best predicted the biochemical recurrence.[57] We can also strengthen the role of RF. Nevertheless, researchers are still divided over which model performs better. Chen et al. found that predicting SVM models was the best,

Table 2
Confusion matrix and classification report for random forest. Classification report for a machine learning model. Table shows the precision, recall, f1-score and support for each class in the dataset. The precision is the ratio of correctly predicted positive observations to the total predicted positive observations. Recall is the ratio of correctly predicted positive observations to the all observations in actual class. F1-score is the harmonic mean of precision and recall. Support is the number of samples of the true response that lie in that class. The accuracy is the ratio of correctly predicted observations to the total observations. Macro average is the unweighted mean of precision, recall and f1-score. Weighted average is the weighted mean of precision, recall and f1-score. The last two rows show how many samples were mislabeled in the training and test sets.

		Precision	Recall	f1-score	Support	Number
	Test dataset	0.77	0.60	0.67	4	
	Training dataset	0.70	0.75	0.77	4	
	Accuracy	–	–	0.72	8	
	Macro average	0.73	0.72	0.72	8	
	Weighted average	0.73	0.72	0.72	8	
Mislabeled in the training set						1
Mislabeled in the test set						2

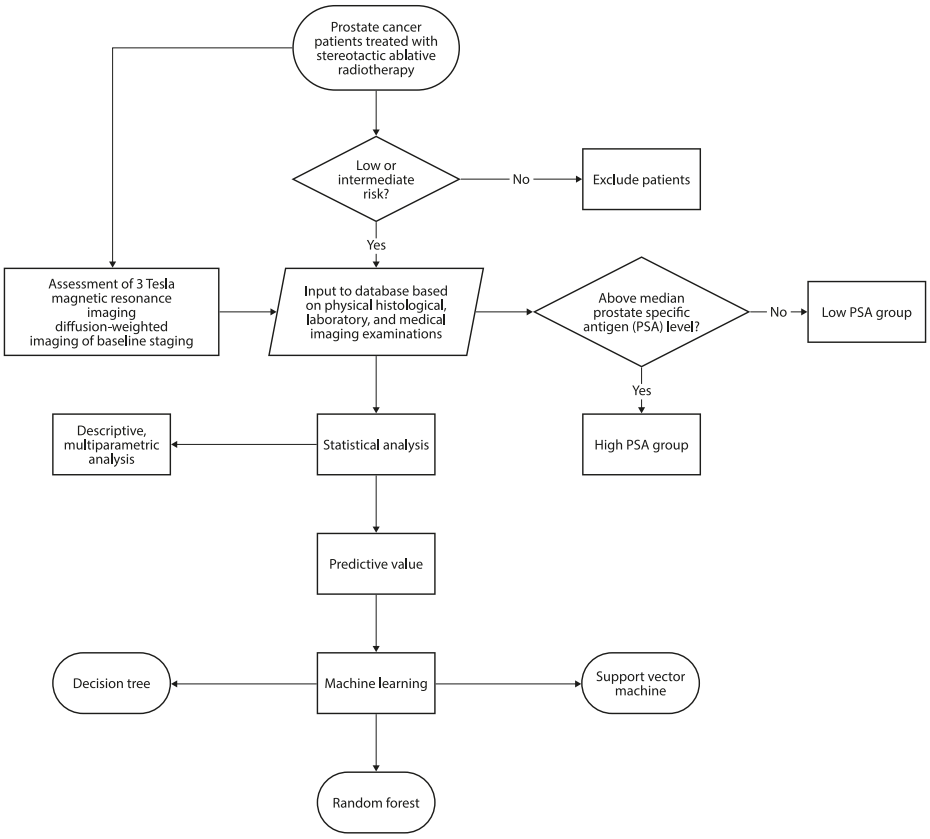

Figure 7. Flow chart of machine learning used for prediction. *prostate-specific antigen (PSA).

followed by RT and DT. Regarding prediction, the researchers discovered that SVM models performed the best, with RT and DT following.[58] Even though SVM may perform better with smaller samples, the low number of elements in our analysis may cause this mismatch.

PSA kinetics are unlikely to be related to baseline ADC values. The curve's trendline indicates a downward trend, but after 12–18 months, a new peak may be visible, followed by a tendency for values to become zero. It is indeed probably because of the effects of androgen therapy, but further research is still needed. Greci et al. found that 3-month PSA density and 3–6 months PSA slope are predictive of long-term freedom from biochemical relapse. However, in our case, we do not find any evidence of the short-term predictive value of these values, nor do we find a correlation between these and 1-year-PSA values.[4]

Several limitations must be acknowledged. The limited number of cases, along with the retrospective nature of the imaging study, represents the main restriction. Although we analyzed the association between pre-treatment DWI and 1-year-PSA values, in SABR the PSA decline is relatively slow. In large series[59] it took a median of 22.6 months. Therefore a repeated analysis of a larger number of patients including PSA kinetics at different time points and the reached lowest value of PSA is warranted. For some machine learning techniques, more than the sample size might be required. Second, the training and test datasets came from the same hospital, necessitating further external validation at different institutions to support the results. Third, our models should be empowered by other possible predictors or variables. Such as positron emission tomography-based uptake values (e.g., metabolic tumor volume [MTV], total lesion glycolysis [TLG]) and their ratios with ADC values might have been included, altogether the dynamic contrast-enhanced magnetic resonance imaging (DCE-MRI) derived volume transfer constant (K^{trans}). Based on our pilot study, we would then broaden our research to examine multicenter data as well as the International Stereotactic Radiosurgery Society (ISRS) European database of SABR patients for additional analysis.

In the future, a larger and more diverse patient cohort can be investigated. The study included a relatively small sample size of 30 patients. A larger and more diverse cohort would provide more robust evidence for the predictive value of diffusion parameters for PSA response in PCa patients treated with SABR. Moreover, validation of independent data would be a great option for future research. To further strengthen the findings, the predictive performance of the machine learning models should be validated on an independent dataset of patients with PCa treated with SABR. This would help to ensure that the results are not specific to the patient population in the original study. The study provided preliminary evidence for the potential of using machine learning to predict PSA response in PCa patients treated with SABR. Future research should focus on developing clinical decision support tools that can incorporate machine learning predictions into patient care.

The first assessment examining a homogeneous group of patients (low-intermediate risk patients treated with SABR) while using DWI was carried out in this study. In addition, as mentioned earlier, the predictive value of the group using machine learning is also being investigated for the first time in this study.

Conclusion

Using our developed, validated, and compared machine learning methods, pre-treatment MRI-DWI values may predict short-term biotherapeutic response in PCa patients treated successfully (without biochemical relapse) with SABR.

The strength of this study is the use of an MRI-DWI parameter, which includes diffusion evaluations. Moreover, ADC_{min} and ADC_{mean} values significantly predicted the clinical outcome; thus, their inclusion in risk stratification may be of additional value for predicting patient treatment outcomes.

Interactive abstract

Conflict of interest statement

The authors declare no conflict of interest.

Key points

Short Title: AI-based prediction of biochemical response using MRI-DWI in PCa.

Question: How can MRI-DWI values predict the outcome of prostate cancer treated with SABR using machine learning?

Pertinent findings: The retrospective study reveals correlations between baseline MR DWI-based parameters (ADC_{min}, ADC_{mean}) and cancer-specific features (iPSA, Volume) and highlights their impact on the biochemical response (low 1-year-PSA, high 1-year-PSA).

Implications for patient care: Clinicians shall measure and implement the evaluation of the suggested parameters (ADC_{min}, ADC_{mean}) to provide the most accurate therapy for the patient.

Author contribution

AMe, YA, FL, and AKe designed the study. OF, AKe collected, segmented, and processed DWI data. FL, AMi, KK, CG, and AKe conducted data collection. AKe provided data processing and visualization. AMe, YA, ZK, and AKe designed, developed, and discussed machine learning scripts. AKe did the statistical analysis and discussed it with AL, ASc, and FL. FL and AKe wrote the paper. AMe, YA, ASc, AL, ASz, BS, DS, AKo, FL, and AKe discussed the results and contributed to the final form of the article. All authors have approved the final copy.

Availability of data and materials, ethics statement

The datasets used and/or analysed during the current study are available from the corresponding author upon reasonable request. Prostate SABR was introduced after national ethical committee approvals (OGYEI: 5838/2017, 66793/2018, 69293/2017).

Acknowledgement

This research did not receive any specific grant from funding agencies in the public, commercial, or not-for-profit sectors.

Appendix A. Supplementary data

Supplementary data to this article can be found online at https://doi.org/10.1016/j.radi.2024.03.015.

References

1. Henley SJ, Ward E, Scott S, Ma J, Anderson RN, Firth AU, et al. *National cancer statistics* 2021;**126**(10):2225–49.
2. Naser-Tavakolian A, Venkataramana A, Spiegel B, Almario C, Kokorowski P, Freedland SJ, et al. The impact of life expectancy on cost-effectiveness of treatment options for clinically localized prostate cancer. *Urol Oncol* 2023;**205**:1–10.
3. Song Y, Xu T. Treatment options for low-risk prostate cancer. *World J Urol Germany* 2022;**40**:2827–8.
4. Greco C, Pares O, Pimentel N, Louro V, Nunes B, Kociolek J, et al. Early PSA density kinetics predicts biochemical and local failure following extreme hypofractionated radiotherapy in intermediate-risk prostate cancer. *Radiother Oncol* 2022;**169**:35–42.
5. Zelefsky MJ, Pinitpatcharalert A, Kollmeier M, Goldman DA, McBride S, Gorovets D, et al. Early tolerance and tumor control outcomes with high-dose ultrahypofractionated radiation therapy for prostate cancer. *Eur Urol Oncol* 2020;**3**(6):748–55.
6. Parikh NR, Kishan AU. Stereotactic body radiotherapy for prostate cancer. *Am J Mens Health* 2020;**14**(3).
7. Cronin KA, Lake AJ, Scott S, Sherman RL, Noone AM, Howlader N, et al. Annual report to the nation on the status of cancer, part I: national cancer statistics. *Cancer* 2018;**124**(13):2785–800.
8. Le Q-T, Shirato H, Giaccia AJ, Koong AC. Emerging treatment paradigms in radiation oncology. *Clin Cancer Res* 2015;**21**(15):3393–401.
9. Palma DA, Olson R, Harrow S, Gaede S, Louie AV, Haasbeek C, et al. Stereotactic ablative radiotherapy versus standard of care palliative treatment in patients with oligometastatic cancers (SABR-COMET): a randomised, phase 2, open-label trial. *Lancet [Internet]* 2019;**393**(10185):2051–8. https://doi.org/10.1016/S0140-6736(18)32487-5.
10. Palma DA, Olson R, Harrow S, Gaede S, Louie AV, Haasbeek C, et al. Stereotactic ablative radiotherapy for the comprehensive treatment of oligometastatic cancers: Long-term results of the SABR-COMET Phase II randomized trial. *J Clin Oncol* 2020;**38**(25):2830–8.
11. Jackson WC, Silva J, Hartman HE, Dess RT, Kishan AU, Beeler WH, et al. Stereotactic body radiation therapy for localized prostate cancer: A systematic review and meta-analysis of over 6,000 patients treated on prospective studies. *Int J Radiat Oncol Biol Phys* 2019;**104**(4):778–89.
12. Valle LF, Lehrer EJ, Markovic D, Elashoff D, Levin-Epstein R, Karnes RJ, et al. A systematic review and meta-analysis of local salvage therapies after radiotherapy for prostate cancer (MASTER). *Eur Urol* 2021;**80**(3):280–92.
13. Johansson B, Olsén JS, Karlsson L, Lundin E, Lennernäs B. High-dose-rate brachytherapy as monotherapy for low- and intermediate-risk prostate cancer: long-term experience of Swedish single-center. *J Contemp Brachytherapy* 2021;**13**(3):245–53.
14. Dinçer S, Uysal E, Berber T, Akboru MH. The efficacy and tolerability of ultrahypofractionated radiotherapy in low-intermediate risk prostate cancer patients: single center experience. *Aging Male* 2021;**24**(1):50–7.
15. Kishan AU, Dang A, Katz AJ, Mantz CA, Collins SP, Aghdam N, et al. Long-term outcomes of stereotactic body radiotherapy for low-risk and intermediate-risk prostate cancer. *JAMA Netw Open* 2019;**2**(2):e188006.
16. Haque W, Butler EB, Teh BS. Stereotactic body radiation therapy for prostate cancer-a review. *Chin Clin Oncol* 2017;**6**(6):1–13.
17. Loblaw A. Stereotactic ablative body radiotherapy for intermediate- or high-risk prostate cancer. *Cancer J (United States)* 2020;**26**(1):38–42.
18. Moon DH, Basak RS, Usinger DS, Gregg A, Morris DE, Perman M, et al. *Health Research Alliance* 2020;**76**(3):391–7.
19. Olson R, Senan S, Harrow S, Gaede S, Louie A, Haasbeek C, et al. Quality of life outcomes after stereotactic ablative radiation therapy (SABR) versus standard of care treatments in the oligometastatic setting: A secondary analysis of the SABR-COMET randomized trial. *Int J Radiat Oncol Biol Phys [Internet]* 2019;**105**(5):943–7. https://doi.org/10.1016/j.ijrobp.2019.08.041.

20. Alayed Y, Davidson M, Quon H, Cheung P, Chu W, Chung HT, et al. Dosimetric predictors of toxicity and quality of life following prostate stereotactic ablative radiotherapy. *Radiother Oncol [Internet]* 2020;**144**:135–40. https://doi.org/10.1016/j.radonc.2019.11.017.
21. Monaco A, Sommer J, Okpara C, Lischalk JW, Haas J, Corcoran A, et al. Comparative results of focal-cryoablation and stereotactic body radiotherapy in the treatment of unilateral, low-to-intermediate-risk prostate cancer. *Int Urol Nephrol* 2022;**54**(10):2529–35.
22. Yamaguchi H, Hori M, Suzuki O, Seo Y, Isohashi F, Yoshioka Y, et al. Clinical significance of the apparent diffusion coefficient ratio in prostate cancer treatment with intensity-modulated radiotherapy. *Anticancer Res* 2016;**36**(12):6551–6.
23. Hegde JV, Demanes DJ, Veruttipong D, Raince J, Park S-J, Raman SS, et al. Pretreatment 3T multiparametric MRI staging predicts for biochemical failure in high-risk prostate cancer treated with combination high-dose-rate brachytherapy and external beam radiotherapy. *Brachytherapy* 2017;**16**(6):1106–12.
24. Onal C, Erbay G, Cem O, Oymak E. The prognostic value of mean apparent diffusion coefficient measured with diffusion-weighted magnetic resonance image in patients with prostate cancer treated with definitive radiotherapy. *Radiother Oncol [Internet]* 2022;**173**:285–91. https://doi.org/10.1016/j.radonc.2022.06.011.
25. Arif M, Schoots IG, Castillo Tovar J, Bangma CH, Krestin GP, Roobol MJ, et al. Clinically significant prostate cancer detection and segmentation in low-risk patients using a convolutional neural network on multi-parametric MRI. *Eur Radiol* 2020;**30**(12):6582–92.
26. Workman C, Jensen LJ, Jarmer H, Berka R, Gautier L, Nielser HB, et al. A new non-linear normalization method for reducing variability in DNA microarray experiments. *Genome Biol* 2002;**3**(9):1–16.
27. Xia H, Akay YM, Akay M. Selecting Relevant Genes from Microarray Datasets Using a Random Forest Model. *IEEE Access* 2021;**9**:97813–21.
28. Parmar C, Grossmann P, Rietveld D, Rietbergen MM, Lambin P, Aerts HJWL. Radiomic machine-learning classifiers for prognostic biomarkers of head and neck cancer. *Front Oncol* 2015;**5**.
29. Wang Y, Shen L, Jin J, Wang G. *Application and Clinical Value of Machine Learning-Based Cervical Cancer Diagnosis and Prediction Model in Adjuvant Chemotherapy for Cervical Cancer : A Single-Center , Controlled , Non-Arbitrary Size Case-Control Study*. 2022. p. 2022.
30. Yang L, Li Z, Liang X, Xu J, Cai Y, Huang C. In: *Radiomic Machine Learning and External Validation Based on 3 . 0 T mpMRI for Prediction of Intraductal Carcinoma of Prostate With Different Proportion*. **12**; 2022. p. 1–9.
31. Wang Z, Tow M, Woon C, Tsang C, Chiong E. Utility of serum biomarkers for predicting cancer in patients with previous neg,ative prostate biopsy. *World J Urol [Internet]* 2022. https://doi.org/10.1007/s00345-022-04085-1.
32. Enderling H, Alfonso JCL, Moros E, Caudell JJ, Harrison LB. Integrating mathematical modeling into the roadmap for personalized adaptive radiation therapy. *Trends Cancer* 2019;**5**(8):467–74.
33. Schwalbe N, Wahl B. Artificial intelligence and the future of global health. *Lancet [Internet]* 2020;**395**(10236):1579–86. https://doi.org/10.1016/S0140-6736(20)30226-9.
34. Deng H, Runger G. Feature selection via regularized trees. *Proceedings of the International Joint Conference on Neural Networks* 2012:10–5.
35. Liu Y-F, Shu X, Qiao X-F, Ai G-Y, Liu L, Liao J, et al. Radiomics-based machine learning models for predicting P504s/P63 immunohistochemical expression: a noninvasive diagnostic tool for prostate cancer. *Front Oncol* 2022;**12**:1–11.
36. Cysouw MCF, Jansen BHE, van de Brug T, Oprea-Lager DE, Pfaehler E, de Vries BM, et al. Machine learning-based analysis of [18F]DCFPyL PET radiomics for risk stratification in primary prostate cancer. *Eur J Nucl Med Mol Imaging* 2021;**48**(2):340–9.
37. Li ZL, Wang HX, Zhang YW, Zhao XH. Random forest–based feature selection and detection method for drunk driving recognition. *Int J Distrib Sens Netw* 2020;**16**(2).
38. Yang L, Xu P, Li M, Wang M, Peng M, Zhang Y, et al. PET/CT Radiomic Features: A Potential Biomarker for EGFR Mutation Status and Survival Outcome Prediction in NSCLC Patients Treated With TKIs. *Front Oncol* 2022;**12**:1–13.
39. Kisivan K, Antal G, Gulyban A, Glavak C, Laszlo Z, Kalincsak J, et al. Triggered imaging with auto beam hold and pre-/posttreatment CBCT during prostate SABR: analysis of time efficiency, target coverage, and normal volume changes. *Pract Radiat Oncol* 2021;**11**(2):e210–8.
40. Jeong JH, Cho IH, Chun KA, Kong EJ, Kwon SD, Kim JH. Correlation between apparent diffusion coefficients and standardized uptake values in hybrid 18F-FDG PET/MR: preliminary results in rectal cancer. *Nucl Med Mol Imaging [Internet]* 2016;**50**(2):150–6. https://doi.org/10.1007/s13139-015-0390-9.
41. Sakane M, Tatsumi M, Kim T, Hori M, Onishi H, Nakamoto A, et al. Correlation between apparent diffusion coefficients on diffusion-weighted MRI and standardized uptake value on FDGPET/ CT in pancreatic adenocarcinoma. *Acta radiol* 2015;**56**(9):1034–41.
42. Yamasaki F, Kurisu K, Satoh K, Arita K, Sugiyama K, Ohtaki M, et al. Apparent diffusion coefficient of human brain tumors at MR imaging. *Radiology* 2005;**235**(3):985–91.
43. Boesen L. Multiparametric MRI in detection and staging of prostate cancer. *Dan Med J* 2017;**64**(2):1–25.
44. Kumar R, Nayyar R, Kumar V, Gupta NP, Hemal AK, Jagannathan NR, et al. Potential of magnetic resonance spectroscopic imaging in predicting absence of prostate cancer in men with serum prostate-specific antigen between 4 and 10 ng/ml: a follow-up study. *Urology* 2008;**72**(4):859–63.
45. Paulus DH, Oehmigen M, Grüneisen J, Umutlu L, Quick HH. Whole-body hybrid imaging concept for the integration of PET/MR into radiation therapy treatment planning. *Phys Med Biol* 2016;**61**(9):3504–20.
46. de Hond AAH, Steyerberg EW, van Calster B. Interpreting area under the receiver operating characteristic curve. *Lancet Digit Health [Internet]* 2022;**4**(12):e853–5. https://doi.org/10.1016/S2589-7500(22)00188-1.
47. Shapiro SS, Wilk MB. An Analysis of Variance Test for Normality (Complete Samples). *Biometrika* 1965;**52**(3/4):591–611.
48. Loblaw A, Liu S, Cheung P. Stereotactic ablative body radiotherapy in patients with prostate cancer. *Transl Androl Urol* 2018;**7**(3):330–40.
49. Correa RJM, Morton G, Chung HT, Tseng C-L, Cheung P, Chu W, et al. Two-fraction stereotactic ablative radiotherapy (SABR) versus two-fraction high dose rate (HDR) brachytherapy for localized prostate cancer: Does dose heterogeneity matter? *Radiother Oncol* 2022;**169**:51–6.
50. Park SY, Kim CK, Park BK, Lee HM, Lee KS. Prediction of biochemical recurrence following radical prostatectomy in men with prostate cancer by diffusion-weighted magnetic resonance imaging: Initial results. *Eur Radiol* 2011;**21**(5):1111–8.
51. Kishan AU, Sun Y, Hartman H, Pisansky TM, Bolla M, Neven A, et al. Androgen deprivation therapy use and duration with definitive radiotherapy for localised prostate cancer: an individual patient data meta-analysis. *Lancet Oncol* 2022;**23**(2):304–16.
52. Kerkmeijer LGW, Groen VH, Pos FJ, Haustermans K, Monninkhof EM, Smeenk RJ, et al. Focal boost to the intraprostatic tumor in external beam radiotherapy for patients with localized prostate cancer: results from the FLAME randomized phase III trial. *J Clin Oncol* 2021;**39**(7):787–96.
53. Hambrock T, Somford DM, Huisman HJ, van Oort IM, Witjes JA, Hulsbergen-van de Kaa CA, et al. Relationship between apparent diffusion coefficients at 3.0-T MR imaging and Gleason grade in peripheral zone prostate cancer. *Radiology* 2011;**259**(2):453–61.
54. Wu X, Reinikainen P, Vanhanen A, Kapanen M, Vierikko T, Ryymin P, et al. Correlation between apparent diffusion coefficient value on diffusion-weighted MR imaging and Gleason score in prostate cancer. *Diagn Interv Imaging [Internet]* 2017;**98**(1):63–71. Available from: https://linkinghub.elsevier.com/retrieve/pii/S2211568416301851.
55. Xie J, Li B, Min X, Zhang P, Fan C, Li Q, et al. Prediction of pathological upgrading at radical prostatectomy in prostate cancer eligible for active surveillance: a texture features and machine learning-based analysis of apparent diffusion coefficient maps. *Front Oncol* 2021;**10**:1–10.
56. Chatterjee A, Turchan WT, Fan X, Griffin A, Yousuf A, Karczmar GS, et al. Can pre-treatment quantitative multi-parametric MRI predict the outcome of radiotherapy in patients with prostate cancer? *Acad Radiol* 2022;**29**(7):977–85.
57. Dutta A, Chan J, Haworth A, Dubowitz DJ, Kneebone A, Reynolds HM. Robustness of magnetic resonance imaging and positron emission tomography radiomic features in prostate cancer: Impact on recurrence prediction after radiation therapy. *Phys Imaging Radiat Oncol [Internet]* 2024;**29**:100530. https://doi.org/10.1016/j.phro.2023.100530.
58. Chen S, Jian T, Chi C, Liang Y, Liang X, Yu Y, et al. Machine learning-based models enhance the prediction of prostate cancer. *Front Oncol* 2022;**12**:1–6.
59. Chen L, Gannavarapu BS, Desai NB, Folkert MR, Dohopolski M, Gao A, et al. Dose-intensified stereotactic ablative radiation for localized prostate cancer. *Front Oncol* 2022;**12**:779182.